Structural Evolution of the $[(CO_2)_n(H_2O)]^-$ Cluster Anions: Quantifying the Effect of Hydration on the Excess Charge Accommodation Motif

Azusa Muraoka,[†] Yoshiya Inokuchi,[†,‡] Nathan I. Hammer,[§,||] Joong-Won Shin,[§,⊥] Mark A. Johnson,[*,§] and Takashi Nagata[*,†]

Department of Basic Science, Graduate School of Arts and Sciences, The University of Tokyo, Komaba, Meguro-ku, Tokyo 153-8902, Japan, and Sterling Chemistry Laboratory, Yale University, P.O. Box 208107, New Haven, Connecticut 06520

Received: April 19, 2009; Revised Manuscript Received: June 25, 2009

The $[(CO_2)_n(H_2O)]^-$ cluster anions are studied using infrared photodissociation (IPD) spectroscopy in the 2800−3800 cm^{-1} range. The observed IPD spectra display a drastic change in the vibrational band features at $n = 4$, indicating a sharp discontinuity in the structural evolution of the monohydrated cluster anions. The $n = 2$ and 3 spectra are composed of a series of sharp bands around 3600 cm^{-1}, which are assignable to the stretching vibrations of H_2O bound to $C_2O_4^-$ in a double ionic hydrogen-bonding (DIHB) configuration, as was previously discussed (*J. Chem. Phys.* **2005**, *122*, 094303). In the $n \geq 4$ spectrum, a pair of intense bands additionally appears at ≈3300 cm^{-1}. With the aid of ab initio calculations at the MP2/6-31+G* level, the 3300 cm^{-1} bands are assigned to the bending overtone and the hydrogen-bonded OH vibration of H_2O bound to CO_2^- via a single O−H···O linkage. Thus, the structures of $[(CO_2)_n(H_2O)]^-$ evolve with cluster size such that DIHB to $C_2O_4^-$ is favored in the smaller clusters with $n = 2$ and 3 whereas CO_2^- is preferentially stabilized via the formation of a single ionic hydrogen-bonding (SIHB) configuration in the larger clusters with $n \geq 4$.

Introduction

When an excess electron is accommodated by a cluster of molecules, the extent of charge delocalization within the aggregate is primarily governed by the competition between stabilization attained by solvent-induced charge localization and the intrinsic tendency toward charge delocalization through resonance interactions. In the case of carbon dioxide, the charge is either localized on a CO_2 monomer or spread over a dimer moiety to form $C_2O_4^-$, and the resulting $(CO_2)_n^-$ cluster anions thus take on an electronic structure represented as either $[CO_2^- \cdot (CO_2)_{n-1}]$ or $[C_2O_4^- \cdot (CO_2)_{n-2}]$.[1−8] These two types of electronic structures, denoted "type I" and "type II", respectively, can be probed with negative-ion photoelectron spectroscopy by taking advantage of the large difference in vertical detachment energy (VDE) between CO_2^- and $C_2O_4^-$, which is essentially retained when these core ions are solvated by the remaining CO_2 neutrals.[3,4,7] Vibrational spectroscopy provides an even more detailed picture of the core ion structures,[8] where a recent report revealed a dramatically size-dependent "core ion switch", in which type I clusters dominate in the intermediate size range $6 \leq n \leq 13$, while the charge-delocalized type II forms are predominant at the smaller sizes $2 \leq n < 6$. The core ion switching behavior of $(CO_2)_n^-$ can be interpreted in the context of the competition between the intrinsic charge delocalization at play in $C_2O_4^-$ and the charge localization (onto CO_2^- monomers) favored when this dimer core ion is exposed to the asymmetrical solvation environments available in the $n = 6 - 13$ size range.[1,8]

The "core ion switch" situation changes drastically when a water molecule is incorporated into $(CO_2)_n^-$.[9−13] In Figure 1, photoelectron spectra of $[(CO_2)_n(H_2O)]^-$ are reproduced along with those of $(CO_2)_n^-$ in the size range $2 \leq n \leq 6$. The comparison clearly shows the earlier onset of type I clusters upon introduction of one H_2O molecule into $(CO_2)_n^-$, demonstrating how a solvent molecule capable of hydrogen bonding can dramatically reduce the size required to induce charge localization onto monomeric CO_2^-. We further explored this effect in an earlier report describing the infrared photodissociation (IPD) spectra of $[(CO_2)_n(H_2O)_m]^-$ ($n = 2$, 3 and $m = 1$, 2) in the 3000−3800 cm^{-1} region.[13] The spectral patterns were analyzed with the aid of ab initio calculations, leading to the identification of the size- and composition-specific structural motifs by which the incorporated H_2O interacts with the core ions. For example, three distinct H-bonding arrangements in the $[(CO_2)_{2,3}(H_2O)]^-$ clusters were identified as depicted in Scheme 1. These motifs, **I-a**, **II-a**, and **II-b**, are all derived from the double ionic hydrogen-bonding (DIHB) configuration, where H_2O interacts with the core ion via donation of two equivalent hydrogen bonds. Motif **I-a** is adopted in the type I structure, while **II-a** and **II-b** correspond to the situation at play in the type II species. Considering the spectral changes evident in Figure 1, we now explore how the local interactions evolve at the critical "crossover" cluster $[(CO_2)_4(H_2O)]^-$ where the system displays both type I and type II behavior in same ion packet.

To address this issue, we have extended the IPD spectral measurements of $[(CO_2)_n(H_2O)]^-$ up to $n = 14$ in the OH stretching region (2800−3800 cm^{-1}). Ab initio MO calculations are also carried out to obtain the optimized geometries,

* Authors to whom correspondence should be addressed: nagata@cluster.c.u-tokyo.ac.jp (T. Nagata), mark.johnson@yale.edu (M. A. Johnson).
† The University of Tokyo.
‡ Present address: Department of Chemistry, Graduate School of Science, Hiroshima University, Kagamiyama, Higashi-Hiroshima, Hiroshima 739-8526, Japan.
§ Yale University.
|| Present address: Department of Chemistry & Biochemistry, The University of Mississippi, P.O. Box 1848, University, MS 38677.
⊥ Present address: Department of Chemistry, Colorado State University, Fort Collins, CO 80523-1872.

10.1021/jp903578e CCC: $40.75
Published on Web 07/15/2009

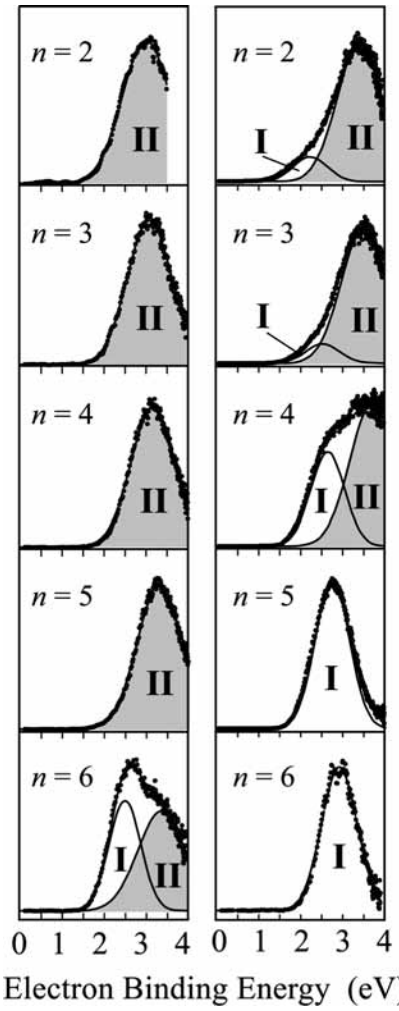

Figure 1. Photoelectron spectra of $(CO_2)_n^-$ (left panel) and $[(CO_2)_n(H_2O)]^-$ (right panel) with $2 \leq n \leq 6$. The spectra are reproduced from ref.[10] The dots represent the experimental data while the solid curves are the best-fit Gaussian profiles. The shaded areas correspond to the band components associated with type II structures. Note that n represents the number of CO_2 molecules in the cluster anions; the total number of constituents is $n + 1$ for $[(CO_2)_n(H_2O)]^-$.

SCHEME 1

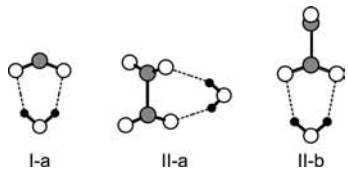

vibrational frequencies, and total energies of $[(CO_2)_n(H_2O)]^-$ for the critical size of $n = 4$. Combining the experimental observations with the ab initio results, we identify the structural motifs appearing in $[(CO_2)_n(H_2O)]^-$ with $n \geq 4$ and discuss the origin of the earlier onset for formation of type I structures in the hydrated cluster anions compared to their nonhydrated analogues.

Experimental Section

The IPD spectra of $[(CO_2)_n(H_2O)]^-$ ($n = 2-10$ and 14) were measured in the 2800−3800 cm^{-1} range using the Yale tandem time-of-flight mass spectrometer.[14] The $[(CO_2)_n(H_2O)]^-$ anions were prepared by electron-impact ionization of free jet. A gas mixture of CO_2 and H_2O was expanded through a pulsed nozzle and bombarded by a counterpropagating 1 keV electron beam, which produced secondary electrons that were efficiently attached to preexisting $[(CO_2)_N(H_2O)_M]$ neutrals. The cluster anions thus produced were mass-analyzed by a time-of-flight mass spectrometer, and species with the *m/e* of interest were isolated by a mass gate. The mass-selected anions were then irradiated by an output of a tunable infrared laser (Nd:YAG-pumped KTP/KTA optical parametric oscillator/amplifier, LaserVision) with an energy of 5 mJ $pulse^{-1}$ and a bandwidth of about 2 cm^{-1}. The infrared excitation resulted in the vibrational predissociation of the cluster anions: $[(CO_2)_n(H_2O)]^- + h\nu \rightarrow [(CO_2)_{n-1}(H_2O)]^- + CO_2$. The resultant fragment ions were mass-analyzed by a reflectron and detected by a microchannel ion detector. The IPD spectra of $[(CO_2)_n(H_2O)]^-$ were obtained by plotting the yields of photofragment ions as a function of the infrared photon energy.

Results and Discussion

A. General Features of IPD Spectra. Figure 2 displays an overview of the IPD spectra of $[(CO_2)_n(H_2O)]^-$ ($n = 2-10$ and 14) measured in the 2800−3800 cm^{-1} range. Although the bands are somewhat better resolved, for $n = 2$ and 3, the features in the 3400−3800 cm^{-1} range are identical to those observed in our previous measurement.[13] The band positions recorded by the two sets of measurements agree quite well with one another: sharp bands appear at 3570 and 3618 cm^{-1} (3570 and 3618 cm^{-1} in the previous study[13]) in the $n = 2$ spectrum, and at 3580 and 3620 cm^{-1} (vs 3577 and 3620 cm^{-1})[13] in $n = 3$ along with a weak hump around 3530 cm^{-1}. In addition to these higher energy features, the larger spectral range available with the present laser system revealed a new series of bands in the 3000−3200 cm^{-1} region (for $n = 2$), and although weaker, they are still discernible in the $n = 3$ spectrum. The $n = 4$ spectrum displays the most complex array of bands of all clusters studied. The overlapping triplet with peaks at 3530, 3590, and 3620 cm^{-1} is reminiscent of the structure found in the $n = 2$ and 3 spectra in this energy range, except for the enhanced intensity of the peak at 3530 cm^{-1}. The $n = 4$ spectrum also exhibits a tiny peak at 2920 cm^{-1}, a sharp peak at 3705 cm^{-1}, and a strong, broad doublet with maxima at 3270 and 3370 cm^{-1}. The $[(CO_2)_n(H_2O)]^-$ species with $n \geq 5$ display almost identical IPD spectral profiles; they consist of a sharp peak at ≈3710 cm^{-1}, broad bands at ≈3270 and ≈3370 cm^{-1}, and tiny peaks at ≈2920, ≈3600, and ≈3650 cm^{-1}. Thus, the IPD spectral features of the $[(CO_2)_n(H_2O)]^-$ species evolve with the cluster size as follows: (1) the $n = 2$ and 3 spectra have almost identical band structures around 3600 cm^{-1}, (2) these are retained in the $n = 4$ spectrum, while new features appear around 3300 cm^{-1} along with peaks at 2920 and 3705 cm^{-1}, (3) the ≈3600 cm^{-1} bands disappear at $n = 5$, whereas the ≈3300 cm^{-1} doublet, along with the 2920 and 3705 cm^{-1} peaks, remain almost intact in the $n = 5$ spectrum, (4) the spectral pattern is essentially constant for $n \geq 5$. From these experimental findings, it can be inferred that the hydrogen-bonded structures formed in the larger $[(CO_2)_n(H_2O)]^-$ clusters are quite different from those occurring in their smaller analogues. The structural change begins promptly at $n = 4$, where previous work[10] established the presence of two types of electronic isomers, $[C_2O_4^- \cdot (CO_2)_{n-2}(H_2O)]^-$ and $[CO_2^- \cdot (CO_2)_{n-1}(H_2O)]^-$, that coexist with comparable populations.

B. Spectral Assignments. ***1. $[(CO_2)_n(H_2O)]^-$ with $n = 2$ and 3.*** The vibrational assignments for the $[(CO_2)_n(H_2O)]^-$ ($n = 2$ and 3) spectra in the 3400−3800 cm^{-1} range have been described in detail in ref.[13] Briefly, the bands are derived from

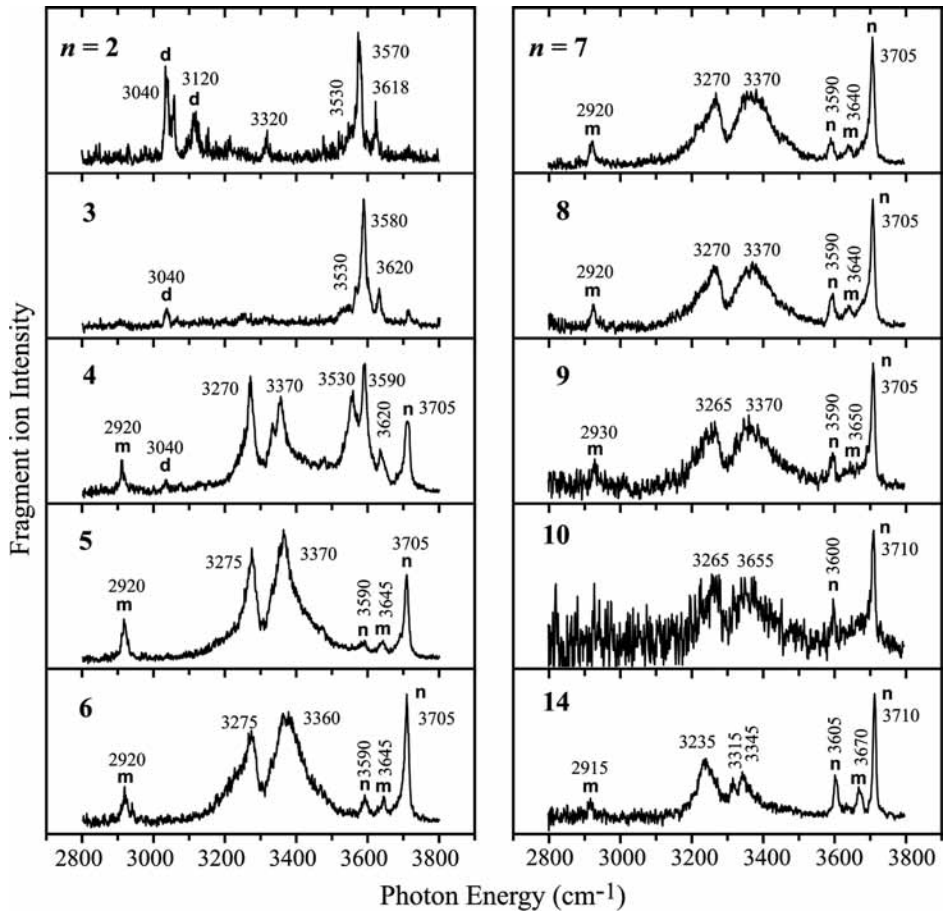

Figure 2. Overview of the infrared photodissociation spectra of $[(CO_2)_n(H_2O)]^-$ with $n = 2-10$, 14 measured in the 2800−3800 cm^{-1} range. The vibrational transitions assignable to the combination bands of $C_2O_4^-$ (dimer core), CO_2^- (monomer core), and CO_2 (neutral solvent) are labeled by "**d**", "**m**", and "**n**", respectively: the 3040 and 3120 cm^{-1} bands (**d**) are assigned to the $\nu_5 + \nu_7$ and $\nu_5 + \nu_7 + \nu_4$ modes of $C_2O_4^-$, 2920 and ≈3650 cm^{-1} (**m**) to $\nu_1 + \nu_3$ and $2\nu_1 + \nu_2 + \nu_3$ of CO_2^-, and ≈3590 and 3705 cm^{-1} (**n**) to $2\nu_2 + \nu_3$ and $\nu_1 + \nu_3$ of CO_2 (ref 8).

water molecules binding to the core ion in a DIHB configuration. In this scheme, the 3570 and 3618 cm^{-1} bands in the $n = 2$ spectrum (3580 and 3620 cm^{-1} in $n = 3$) are assigned respectively to the symmetric and asymmetric OH stretching vibrations of the H_2O molecule forming the ring structure with $C_2O_4^-$ (motif **II-a** or **II-b**). The weaker hump around 3530 cm^{-1} is less clear, and has been ascribed to the symmetric OH stretching vibration of the H_2O molecule that participates in the formation of a ring structure with CO_2^- (motif **I-a**). For readers' convenience, Figure 3 reproduces the optimized structures for $[(CO_2)_{2,\ 3}(H_2O)]^-$ isomers which were identified as the IPD spectral carriers in the previous study.[11,13]

The new series of bands observed in the lower energy 3000−3200 cm^{-1} range closely resemble those observed in the IPD spectrum of $(CO_2)_3^-$,[8] and are thus associated with the dimer anion known[10] to be the core ion in $[(CO_2)_{2,\ 3}(H_2O)]^-$. Specifically, these are assigned to combination bands involving the $\nu_5 + \nu_7 + x\nu_4$ ($x = 0$ and 1) modes of $C_2O_4^-$ which are remarkably unperturbed when the ion is coordinated directly to a water molecule.

2. $[(CO_2)_n(H_2O)]^-$ with $n = 4$. On the basis of the above discussion of the $n = 2$ and 3 spectra, assignment of the $[(CO_2)_4(H_2O)]^-$ vibrational bands around 3600 cm^{-1} is straightforward. The 3590 and 3620 cm^{-1} bands can be traced to the symmetric and the asymmetric OH stretching vibrations of an H_2O molecule involved in the ring structure composed of $C_2O_4^-$ and H_2O (**II-a** and **II-b** in Scheme 1), while the 3530 cm^{-1} band appears in the location of the symmetric OH stretching vibration of H_2O bound to a CO_2^- monomer core in a DIHB manner (**I-a**). The enhanced relative contribution of the 3530 cm^{-1} band then suggests an increasing population of $[(CO_2)_4(H_2O)]^-$ isomers containing motif **I-a**. Assignment of the 2920 and 3705 cm^{-1} bands is also straightforward based on comparison with IPD spectrum of $(CO_2)_n^-$,[8] where similar features occur and are identified as the $\nu_1 + \nu_3$ combination bands of CO_2^- and CO_2, respectively. Once again, the $\nu_5 + \nu_7 + x\nu_4$ combination bands of $C_2O_4^-$ are weak but evident in the 3000−3200 cm^{-1} range. These assignments are consistent with the fact that $CO_2^-\cdot(CO_2)_3(H_2O)$ and $C_2O_4^-\cdot(CO_2)_2(H_2O)$ isomeric forms are coexisting in $[(CO_2)_4(H_2O)]^-$.

The other dominant feature of the $n = 4$ spectrum is the broad doublet emerging around 3300 cm^{-1}. A key to the assignment of this structure is its strong resemblance to the pattern found in $[(CO_2)_1(H_2O)_2]^-$ (3249 and 3345 vs 3270 and 3370 cm^{-1}) where it was traced[13] to the overtone of the bending and hydrogen-bonded OH stretching vibrations of the H_2O molecules, which are independently bound to the O atoms of CO_2^-. We can therefore infer that one of the $[(CO_2)_4(H_2O)]^-$ isomers contains a structural motif where H_2O interacts with CO_2^- only via a single hydrogen bond (SIHB configuration). We next turn to ab initio calculations to further explore this possibility.

Ab initio MO calculations for $[(CO_2)_4(H_2O)]^-$ were performed by using the GAUSSIAN98 program package.[15] Geometry optimizations and vibrational analyses were carried out at the MP2/6-31+G* level. In order to compare the calculated vibrational transition energies with the observed spectra, a

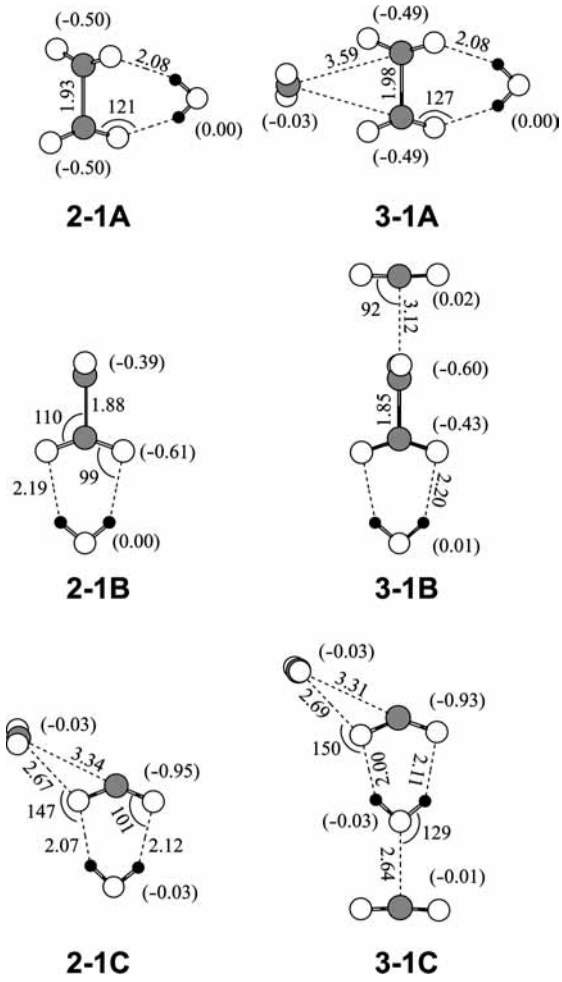

Figure 3. Geometries of $[(CO_2)_{2,3}(H_2O)]^-$ optimized at the MP2/6-311++G** level (taken from refs 11 and13). In referring to each isomeric form, the first digit of the notation "***n-m*X**" represents the number ***n*** of CO_2 molecules involved in the cluster anion, the second digit the number ***m*** of H_2O molecules, and the last character "**X**" is for identifying the individual structure. Bond lengths and angles are given in units of angstroms and degrees. Net Mulliken charge populations for the constituent molecules are included in parentheses for each isomeric form.

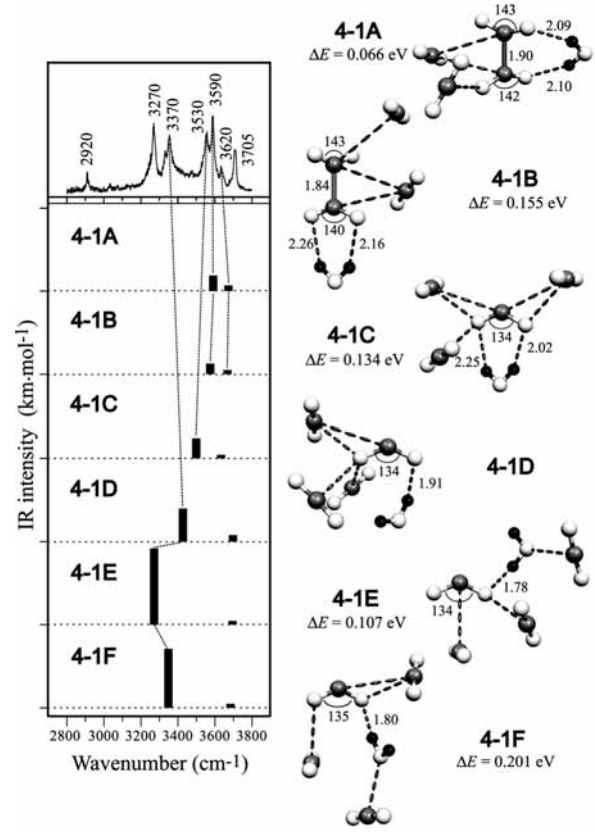

Figure 4. IPD spectra of $[(CO_2)_4(H_2O)]^-$ (top panel) compared with the stick diagrams of the calculated harmonic vibrational frequencies for the $[(CO_2)_4(H_2O)]^-$ isomeric forms optimized at the MP2/6-31+G* level. One unit in the ordinate corresponds to the IR intensity of 1000 km·mol^{-1}. Also shown on the right side are the corresponding optimized structures of the $[(CO_2)_4(H_2O)]^-$ isomers. Isomers **4-1A**−**4-1F** are the most stable representatives among those having the same hydrogen-bonding motifs.

SCHEME 2

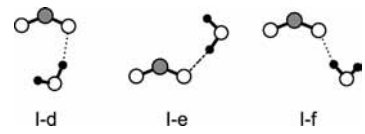

scaling factor of 0.9696 was employed. This factor was determined so as to reproduce the OH stretching frequencies of an isolated H_2O molecule. In Figure 4, the observed IPD spectrum is compared with the calculated vibrational patterns along with the optimized geometries for $[(CO_2)_4(H_2O)]^-$, which can be classified systematically into six groups according to their structural motifs. The present MP2 calculations actually recovered 24 stable isomeric forms for $[(CO_2)_4(H_2O)]^-$, and the optimized structures displayed in Figure 4 correspond to the lowest-energy representatives of each group. Among these six isomeric forms, thee (**4-1A**−**4-1C**) possess a DIHB configuration (motifs **I-a**, **II-a**, and **II-b**), and species **4-1A**−**4-1C** could account for the higher energy OH stretching bands observed at 3530, 3590, and 3620 cm^{-1}. The other three forms (**4-1D**−**4-1F**) have an SIHB configuration, where the H_2O molecule is hydrogen-bonded to CO_2^- through a single O−H···O linkage. The calculated vibrational patterns for **4-1D**−**4-1F** exhibit an intense transition in the 3300−3400 cm^{-1} range, which arises from the hydrogen-bonded OH stretching vibration of H_2O, thus accounting for the 3370 cm^{-1} band. On the analogy of the $[(CO_2)_n(H_2O)_2]^-$ ($n = 1-3$) case, the 3270 cm^{-1} band is ascribed to the overtone of the H_2O bending vibration,[13] the intensity of which is enhanced via resonance coupling with the 3370 cm^{-1} transition. Although the vibrational frequency predicted for the hydrogen-bonded OH stretching vibration in **4-1E** (3271 cm^{-1}) is in excellent agreement with the observed frequency (3270 cm^{-1}) this could be coincidental given the expected accuracy of the calculations. Theory also predicts a weak band around 3700 cm^{-1} for **4-1D**−**4-1F**, which corresponds to the free OH stretching vibration of the hydrogen-bonded H_2O, but this feature would probably be lost due to overlap with the ($\nu_1 + \nu_3$) combination band of CO_2 at 3705 cm^{-1}. Analysis of the minimum energy structures reveals three anionic H-bonding structural motifs first appearing at $n = 4$, which are denoted **I-d**, **I-e**, and **I-f**, respectively in Scheme 2.

Of course, the assignment of the doublet to a Fermi-resonance interaction can be directly tested by isotopic substitution. Therefore, to reinforce the above argument, we have also examined the IPD spectra of isotopic-substituted species, $[(CO_2)_4(HDO)]^-$ and $[(CO_2)_4(D_2O)]^-$. The resulting spectra are shown in Figure 5, and the twin peaks around 3300 cm^{-1} indeed collapse into a single broad feature in $[(CO_2)_4(HDO)]^-$ before disappearing in $[(CO_2)_4(D_2O)]^-$. This evolution is easily understood on the basis of the ab initio results also shown in Figure

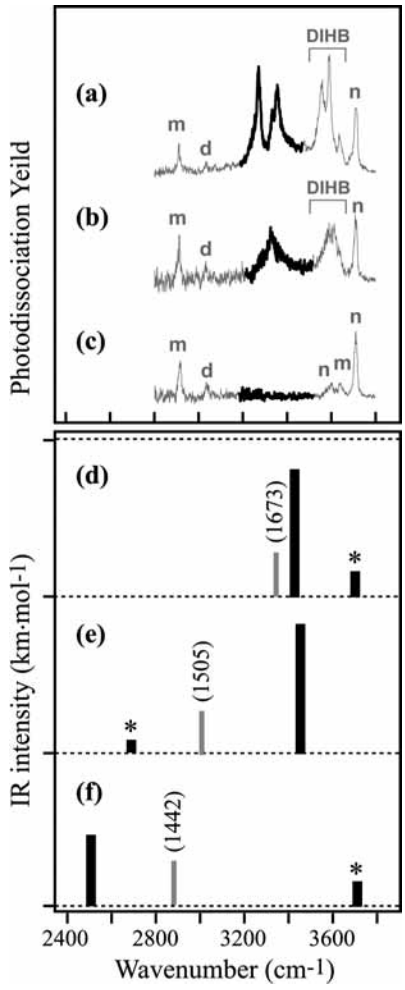

Figure 5. IPD spectra of the isotopically substituted cluster anions with $n = 4$ (upper panel): (a) $[(CO_2)_4(H_2O)]^-$, (b) $[(CO_2)_4(HDO)]^-$, and (c) $[(CO_2)_4(D_2O)]^-$. The spectral regions for the hydrogen-bonded OH stretching vibrations of an SIHB water molecule are highlighted in thick lines. As in Figure 2, the vibrational bands ascribable to $C_2O_4^-$, CO_2^-, and CO_2 in the $n = 4$ anions are labeled by "**d**", "**m**", and "**n**", respectively. Those indicated by "**DIHB**" are the vibrational bands for the hydrogen-bonded OH stretching modes of H_2O involved in a DIHB configuration. In the lower panel, also shown for comparison are the calculated frequencies of the OH vibrations in (d) $(CO_2)_3 \cdot CO_2^- \cdots H-OH$, (e) $(CO_2)_3 \cdot CO_2^- \cdots H-OD$, and (f) $(CO_2)_3 \cdot CO_2^- \cdots D-OH$ taking on the global minimum configuration **4-1D**. One unit in the ordinate corresponds to the IR intensity of 500 km·mol^{-1}. The frequency calculations are performed at the MP2/6-31+G* level. Scaling factors for the calculated vibrational frequencies are 0.9486 for the HOH bending vibration and 0.9696 for the OH stretching vibrations in $[(CO_2)_4(H_2O)]^-$, 0.9515 for the HOD bending vibrations, and 0.9751 for the OH/OD stretching vibrations in $[(CO_2)_4(HDO)]^-$. These factors are determined so as to reproduce the normal-mode frequencies of an isolated H_2O isotopomer. The tallest stick in each calculated spectrum corresponds to the hydrogen-bonded OH (OD) stretching vibration. The sticks marked with asterisks correspond to the free OH (OD) vibrations. The narrow sticks in gray indicate the frequency positions for the (harmonic) $2\nu_2$ bending overtone along with the calculated ν_2 frequencies in parentheses.

5, where the stick diagrams of the calculated vibrational frequencies are displayed for the two isotopomers arising from the singly deuterated **4-1D** species. In discussion of the results in Figure 5, the essential features are the frequencies of the $2\nu_2$ bending overtones relative to the H-bonded OH stretches, given a mixing matrix element close to 35 cm^{-1}.[16] The $2\nu_2$ transition is calculated to be close enough to interact with the hydrogen-bonded OH stretching vibration in $(CO_2)_3 \cdot CO_2^- \cdots H-OH$, while this is not the case in both $(CO_2)_3 \cdot CO_2^- \cdots H-OD$ and $(CO_2)_3 \cdot CO_2^- \cdots D-OH$. These results are thus consistent with assignment of the doublet to resonance coupling between the hydrogen-bonded OH stretching vibration and the $2\nu_2$ bending overtone in normal $[(CO_2)_4(H_2O)]^-$ species.

The total energies of the $[(CO_2)_4(H_2O)]^-$ local minima were evaluated by carrying out single-point energy calculations at the CCSD(T)/6-31+G* level with the optimized structures obtained in the MP2/6-31+G* calculations (CCSD(T)/6-31+G*//MP2/6-31+G*). Structure **4-1D** is recovered as the global minimum with an energy ordering as follows:

4-1D < **4-1A**($\Delta E = 0.07$ eV) < **4-1E**(0.11) < **4-1C**(0.13) < **4-1B**(0.16) < **4-1F**(0.20)

Note that **4-1D** is a type I structure (CO_2^- core), in contrast to the $[(CO_2)_{2,3}(H_2O)]^-$ cases, where the most stable isomeric forms, **2-1A** and **3-1A**, both have type II structures with a $C_2O_4^-$ core.

3. $[(CO_2)_n(H_2O)]^-$ with $n \geq 5$. The IPD spectra for $n \geq 5$ are simpler than those for $n < 5$ and are consistent with a scenario where they all occur as type I isomers best represented as $[CO_2^- \cdot (CO_2)_{n-1}(H_2O)]$ (see Figure 1). We could not attempt ab initio calculations for these larger species as they are both computationally too demanding and occur with increasingly complex potential surfaces giving rise to large numbers of local minima. However, the persistence of the bands already present in the type I form of the $n = 4$ cluster, together with the absence of any new features emerging at larger size, are based on the **I-d**, **I-e**, and **I-f** structural subunits, which give rise to the two prominent peaks in the 3500 cm^{-1} region through the resonant coupling mechanism between the HOH bend overtone and the bound OH stretch fundamental. As in the case of $n = 4$, the 2920 and 3705 cm^{-1} bands are assigned to the combination of $\nu_1 + \nu_3$ of CO_2^- and CO_2, respectively. A pair of weak bands are now clearly resolved around 3600 cm^{-1}, which are evident because of the absence of the overlapping high energy bands arising from type II structures. These were observed in the previous study of $(CO_2)_n^-$; the 3590 cm^{-1} band is due to the $2\nu_2 + \nu_3$ combination of CO_2 while the 3645 cm^{-1} feature is traced to the $\nu_1 + \nu_2 + \nu_3$ mode of CO_2^-.[8] The relative intensities of the 3590 and 3705 cm^{-1} bands tend to increase with cluster size as can be anticipated from the increasing numbers of CO_2 solvent molecules.

C. Structural Evolution in $[(CO_2)_n(H_2O)]^-$. On the basis of the findings described above, we are now in a position to discuss the structural evolution in $[(CO_2)_n(H_2O)]^-$. First, let us summarize the core ion formation and hydration motifs occurring in $[(CO_2)_n(H_2O)]^-$. For the $n = 2$ and 3 species, the dominant isomers take on type II structures ($C_2O_4^-$ cores) containing motifs **II-a** and **II-b**. The type I isomer (CO_2^- core) with motif **I-a** is only a minor species at $n = 2$ and 3. All these structural motifs, **I-a**, **II-a**, and **II-b**, belong to the DIHB configuration. At $n = 4$, the type I and II isomers have comparable populations.[10] The increase in the type I population introduces new isomeric forms having motifs **I-d**−**I-f**. All these can be characterized as "open" structures with SIHB configurations, where the CO_2^- ion core interacts with H_2O through a single O−H···O hydrogen bond. For the larger clusters with $n \geq 5$, only type I isomers appear which retain the spectral signatures of the **I-d**−**I-f** motifs. It is important to note that ab initio calculations predict many isomeric forms that exhibit similar local hydration motifs but differ according to their overall geometries. As these have almost identical vibrational patterns,

we have highlighted isomeric forms **4-1D**−**4-1F** as representatives of the spectral carriers on the basis that they are recovered as low energy forms within this class.

The present findings raise the naive question of whether we can identify the leading factors that contribute to the structural evolution in $[(CO_2)_n(H_2O)]^-$. Generally, ionic systems gain their stabilization energies by charge delocalization through resonance interactions (when available) and/or by electrostatic interactions with surrounding solvents. In the smaller $[(CO_2)_n(H_2O)]^-$ clusters such as the $n = 2$ and 3 species, only a restricted number of molecules are available for solvation and, consequently, the excess charge tends to be delocalized over two CO_2 molecules through the charge-resonance interaction, resulting in a type II structure. As the excess charge is delocalized equally on the terminal O atoms in $C_2O_4^-$,[1] H_2O interacts with the $C_2O_4^-$ core as it tends to do with large excess charge distributions, i.e., through formation of the DIHB configuration. This inference is supported quantitatively by the ab initio results which indicate that **2-1A** and **3-1A** (Figure 3) are the global minimum structures for $n = 2$ and 3.[11,13] It should be also noted that the separation between the terminal oxygen atoms of the $C_2O_4^-$ core is calculated to be 2.96 Å in **2-1A** and 3.02 Å in **3-1A**,[17] which provides favorable binding sites for stable DIHB configurations.[18] Hence, the $C_2O_4^- \cdot H_2O$ component assembles predominantly with a DIHB configuration in $[(CO_2)_{2,\ 3}(H_2O)]^-$. When the cluster size is increased, the number of solvent molecules increases and, as a result, stabilization due to solvation begins to make a dominant contribution. Intuitively, the system gains a larger amount of solvation energy through the electrostatic interactions when a larger number of neutral molecules occupy the solvation sites around the core ion. As discussed at length in the context of charge localization in the homogeneous $(CO_2)_n^-$ system,[8] asymmetrical solvation induces charge localization onto a single CO_2^- molecule. When this occurs, the distance between the oxygen atoms is too small to support the DIHB motif, and the monohydrate adopts an SIHB configuration. The present experimental results indicate that this situation is first achieved at $n = 4$ with the **4-1D** configuration, as also revealed by the ab initio energy ordering, and that the situation does not change in the larger $[(CO_2)_n(H_2O)]^-$ clusters with $n \geq 5$.

It is interesting to compare the "core ion switch" behavior shown in $[(CO_2)_n(H_2O)]^-$ with those in $(CO_2)_n^-$ and $[(CO_2)_n(CH_3OH)]^-$ in terms of the minimum cluster size at which type I becomes predominant. When the total number of constituent molecules are counted, the minimum size is 6 for $(CO_2)_n^-$,[3] 5 for $[(CO_2)_n(H_2O)]^-$,[10] and 3 for $[(CO_2)_n(CH_3OH)]^-$.[10,19] According to the previous discussion on the origin of the core ion switch,[8] the driving force for promoting the CO_2^- formation is traced to the asymmetric solvation environment surrounding the core ion. In the $(CO_2)_n^-$ case, solvent asymmetry arises from the incompleteness of the first solvation shell in the size range $6 \leq n \leq 13$. In contrast, solvation shells intrinsically occur asymmetrically in the heterogeneous $[(CO_2)_n(H_2O)]^-$ and $[(CO_2)_n(CH_3OH)]^-$ clusters. Taking into consideration the fact that type I isomers appear as major species even at $n = 2$ in the $[(CO_2)_n(CH_3OH)]^-$ case,[10] we infer that the local aspects of the H-bonding interaction in $[(CO_2)_n(CH_3OH)]^-$ become a main cause for charge localization. That is, since methanol can only donate one H-bond, the DIHB arrangement that is preferred for type II clusters is not available. Seen from this viewpoint, the present $[(CO_2)_n(H_2O)]^-$ results suggest that the ability of H_2O to form a DIHB configuration allows the type II forms to persist to larger size in the hydrates. It is not until $n = 4$ that the neutral CO_2 solvent molecules overpower this intrinsic type II motif and drive the system toward charge localized clusters with type I cores.

Conclusion

In summary, we report infrared photodissociation (IPD) spectra of $[(CO_2)_n(H_2O)]^-$ ($n = 2-10$, 14) in the 2800−3800 cm^{-1} range and interpret the results with ab initio calculations. The observed IPD spectra can be classified into two groups according to their patterns of hydrogen-bonded OH stretching vibrations. The $n = 2$ and 3 spectra are characterized by a series of sharp bands around 3600 cm^{-1}, whereas the $n > 4$ spectra are dominated exclusively by a broad doublet around 3300 cm^{-1} along with transitions arising from neutral CO_2 and the CO_2^- core ion. Interestingly, both groups of bands appear in the $n = 4$ spectrum. This new spectroscopic information confirms the previous conclusions based on photoelectron specctroscopy[10,12] that type II isomers ($C_2O_4^-$ core) are preferably formed in $[(CO_2)_{2,3}(H_2O)]^-$ while type I isomers (CO_2^- core) become dominant in $[(CO_2)_n(H_2O)]^-$ with $n > 4$; both types coexist at $n = 4$. The band patterns provide more precise information on the hydrogen-bonding structures at play, where the $[(CO_2)_{2,3}(H_2O)]^-$ clusters occur with both hydrogen atoms of the water molecule engaged in anionic hydrogen bonds, and the larger clusters $[(CO_2)_{n>4}(H_2O)]^-$ occur with the single anionic H-bonding motif. Through the structural evolution shown in $[(CO_2)_n(H_2O)]^-$, H_2O demonstrates its ability to bridge across the charge-delocalized $C_2O_4^-$ core ion, acting to reinforce the dimer structure, as well as contribute to the destruction of the dimer by tightly binding to one of the constituents, causing charge localization onto the CO_2^- monomer core ion.

Acknowledgment. The authors are grateful to Professor K. Takatsuka for the loan of high-performance computers. A part of the ab initio calculations was performed by using the computer systems at Research Center for Computational Science, Okazaki Research Facilities, National Institutes of Natural Sciences (NINS). This work is partly supported by Grants-in-Aid for Scientific Research (Grants 18550007, 19029011, and 20038015) from the Japan Society for the Promotion of Science (JSPS) and from the Ministry of Education, Culture, Sports, Science and Technology (MEXT). M.A.J. thanks the Department of Energy for support of this work under Grant DE-FG02-06ER15800.

Supporting Information Available: Structure parameters for the $[(CO_2)_4(H_2O)]^-$ isomeric forms shown in Figure 4 (MP2/6-31+G*). The material is available free of charge via the Internet at http://pubs.acs.org. The structure parameters for all the $[(CO_2)_4(H_2O)]^-$ isomers obtained in the present study are available from the authors on request.

References and Notes

(1) Fleischman, S. H.; Jordan, K. D. *J. Phys. Chem.* **1987**, *91*, 1300.
(2) Bowen, K. H.; Eaton, J. G. In *The Structure of Small Molecules and Ions*; Naaman, R., Vagar, Z., Eds.; Plenum Press: New York, 1987; p 147.
(3) DeLuca, M. J.; Niu, B.; Johnson, M. A. *J. Chem. Phys.* **1988**, *88*, 5857.
(4) Tsukuda, T.; Johnson, M. A.; Nagata, T. *Chem. Phys. Lett.* **1997**, *268*, 429.
(5) Saeki, M.; Tsukuda, T.; Nagata, T. *Chem. Phys. Lett.* **2001**, *340*, 376.
(6) Sommerfeld, T.; Posset, T. *J. Chem. Phys.* **2003**, *119*, 7714.
(7) Mabbs, R.; Surber, E.; Velarde, L.; Sanov, A. *J. Chem. Phys.* **2004**, *120*, 5148.

(8) Shin, J.-W.; Hammer, N. I.; Johnson, M. A.; Schneider, H.; Glöβ, A.; Weber, J. M. *J. Phys. Chem. A* **2005**, *109*, 3146.
(9) Nagata, T.; Yoshida, H.; Kondow, T. *Chem. Phys. Lett.* **1992**, *199*, 205.
(10) Tsukuda, T.; Saeki, M.; Kimura, R.; Nagata, T. *J. Chem. Phys.* **1999**, *110*, 7846.
(11) Saeki, M.; Tsukuda, T.; Iwata, S.; Nagata, T. *J. Chem. Phys.* **1999**, *111*, 6333.
(12) Surber, E.; Mabbs, R.; Habteyes, T.; Sanov, A. *J. Phys. Chem. A* **2005**, *109*, 4452.
(13) Muraoka, A.; Inokuchi, Y.; Nishi, N.; Nagata, T. *J. Chem. Phys.* **2005**, *122*, 094303.
(14) Johnson, M. A.; Lineberger, W. C. In *Techniques in Chemistry*; Farrar, J. M., Saunders, W. H., Eds.; Wiley: New York, 1988; Vol. 20, p 591.
(15) Frisch, M. J.; Trucks, G. W.; Schlegel, H. B.; Scuseria, G. E.; Robb, M. A.; Cheeseman, J. R.; Zakrzewski, V. G.; Montgomery, J. A., Jr., Stratmann, R. E.; Burant, J. C.; Dapprich, S.; Millam, J. M.; Daniels, A. D.; Kudin, K. N.; Strain, M. C.; Farkas, O.; Tomasi, J.; Barone, V.; Cossi, M.; Cammi, R.; Mennucci, B.; Pomelli, C.; Adamo, C.; Clifford, S.; Ochterski, J.; Petersson, G. A.; Ayala, P. Y.; Cui, Q.; Morokuma, K.; Rega, N.; Salvador, P.; Dannenberg, J. J.; Malick, D. K.; Rabuck, A. D.; Raghavachari, K.; Foresman, J. B.; Cioslowski, J.; Ortiz, J. V.; Baboul, A. G.; Stefanov, B. B.; Liu, G.; Liashenko, A.; Piskorz, P.; Komaromi, I.; Gomperts, R.; Martin, R. L.; Fox, D. J.; Keith, T.; Al-Laham, M. A.; Peng, C. Y.; Nanayakkara, A.; Challacombe, M.; Gill, P. M. W.; Johnson, B.; Chen, W.; Wong, M. W.; Andres, J. L.; Gonzalez, C.; Head-Gordon, M.; Replogle, E. S. Pople J. A. *Gaussian 98, Revision A.11.4* Gaussian, Inc.: Pittsburgh, PA, 2002.
(16) Robertson, W. H.; Weddle, G. H.; Kelley, J. A.; Johnson, M. A. *J. Phys. Chem. A* **2002**, *106*, 1205.
(17) Muraoka, A. Ph. D. Dissertation, The University of Tokyo, 2005.
(18) Robertson, W. H.; Price, E. A.; Weber, J. M.; Shin, J.-W.; Weddle, G. H.; Johnson, M. A. *J. Phys. Chem. A* **2003**, *107*, 6527.
(19) Muraoka, A.; Inokuchi, Y.; Nagata, T. *J. Phys. Chem. A* **2008**, *112*, 4906.

JP903578E